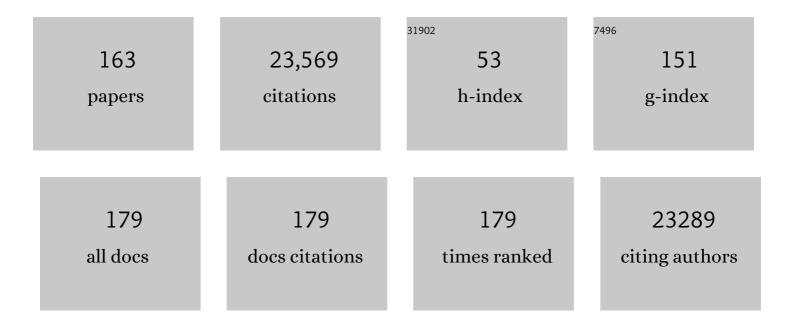
## Zhenhai Xia

List of Publications by Year in descending order

Source: https://exaly.com/author-pdf/2816897/publications.pdf Version: 2024-02-01



Ζηένηνα Χιν

#	Article	IF	CITATIONS
1	Syntheses, mechanisms, and applications of bio-inspired self-cleaning surfaces. , 2022, , 367-392.		1
2	Highly efficient and selective electrocatalytic hydrogen peroxide production on Co-O-C active centers on graphene oxide. Communications Chemistry, 2022, 5, .	2.0	33
3	Eutectic dual-phase microstructure modulated porous high-entropy alloys as high-performance bifunctional electrocatalysts for water splitting. Journal of Materials Chemistry A, 2022, 10, 11110-11120.	5.2	18
4	Fe, V-co-doped C2N for electrocatalytic N2-to-NH3 conversion. Journal of Energy Chemistry, 2021, 53, 303-308.	7.1	55
5	Tailoring nanoprecipitates for ultra-strong high-entropy alloys via machine learning and prestrain aging. Journal of Materials Science and Technology, 2021, 69, 156-167.	5.6	48
6	Catalytic mechanism and design principle of coordinately unsaturated single metal atom-doped covalent triazine frameworks with high activity and selectivity for CO <sub>2</sub> electroreduction. Journal of Materials Chemistry A, 2021, 9, 3555-3566.	5.2	26
7	Multiscale Manufacturing of Amorphous Alloys by a Facile Electrodeposition Approach and Their Property Dependence on the Local Atomic Order. ACS Applied Materials & Interfaces, 2021, 13, 9260-9271.	4.0	10
8	Carbon-supported layered double hydroxide nanodots for efficient oxygen evolution: Active site identification and activity enhancement. Nano Research, 2021, 14, 3329-3336.	5.8	14
9	CrN-Encapsulated Hollow Cr-N-C Capsules Boosting Oxygen Reduction Catalysis in PEMFC. CCS Chemistry, 2021, 3, 208-218.	4.6	28
10	The effect of local atomic configuration in high-entropy alloys on the dislocation behaviors and mechanical properties. Materials Science & Engineering A: Structural Materials: Properties, Microstructure and Processing, 2021, 815, 141253.	2.6	18
11	Designing Undercoordinated Ni–N <sub><i>x</i></sub> and Fe–N <sub><i>x</i></sub> on Holey Graphene for Electrochemical CO <sub>2</sub> Conversion to Syngas. ACS Nano, 2021, 15, 12006-12018.	7.3	68
12	Bioinspired Smart Materials With Externally-Stimulated Switchable Adhesion. Frontiers in Nanotechnology, 2021, 3, .	2.4	2
13	Insights of Heteroatoms Dopingâ€Enhanced Bifunctionalities on Carbon Based Energy Storage and Conversion. Advanced Functional Materials, 2021, 31, 2009109.	7.8	58
14	Rational design of boron-containing co-doped graphene as highly efficient electro-catalysts for the nitrogen reduction reaction. Journal of Materials Chemistry A, 2021, 9, 24590-24599.	5.2	14
15	Unraveling the Structural Statistics and Its Relationship with Mechanical Properties in Metallic Glasses. Nano Letters, 2021, 21, 9108-9114.	4.5	9
16	A Tough Reversible Biomimetic Transparent Adhesive Tape with Pressure-Sensitive and Wet-Cleaning Properties. ACS Nano, 2021, 15, 19194-19201.	7.3	20
17	Atomistic simulations on nanoimprinting of copper by aligned carbon nanotube arrays under a high-frequency mechanical vibration. Nanotechnology, 2020, 31, 045303.	1.3	3
18	N-doping induced tensile-strained Pt nanoparticles ensuring an excellent durability of the oxygen reduction reaction. Journal of Catalysis, 2020, 382, 247-255.	3.1	61

#	Article	IF	CITATIONS
19	Reducedâ€Grapheneâ€Oxideâ€Guided Directional Growth of Planar Lithium Layers. Advanced Materials, 2020, 32, e1907079.	11.1	70
20	Core effect of local atomic configuration and design principles in AlxCoCrFeNi high-entropy alloys. Scripta Materialia, 2020, 178, 181-186.	2.6	29
21	Electronic coupling strategy to boost water oxidation efficiency based on the modelling of trimetallic hydroxides Ni1-x-yFexCry(OH)2: From theory to experiment. Chemical Engineering Journal, 2020, 402, 126144.	6.6	11
22	Transforming active sites in nickel–nitrogen–carbon catalysts for efficient electrochemical CO2 reduction to CO. Nano Energy, 2020, 78, 105213.	8.2	69
23	Enhancing both selectivity and activity of CO2 conversion by breaking scaling relations with bimetallic active sites anchored in covalent organic frameworks. Journal of Catalysis, 2020, 390, 126-134.	3.1	41
24	Deformation mechanism in Al <sub>0.1</sub> CoCrFeNi Σ3(111)[11̄0] high entropy alloys – molecular dynamics simulations. RSC Advances, 2020, 10, 27688-27696.	1.7	16
25	Hole-punching for enhancing electrocatalytic activities of 2D graphene electrodes: Less is more. Journal of Chemical Physics, 2020, 153, 074701.	1.2	2
26	A universal descriptor based on p <sub>z</sub> -orbitals for the catalytic activity of multi-doped carbon bifunctional catalysts for oxygen reduction and evolution. Nanoscale, 2020, 12, 19375-19382.	2.8	28
27	Disperse Multimetal Atom-Doped Carbon as Efficient Bifunctional Electrocatalysts for Oxygen Reduction and Evolution Reactions: Design Strategies. Journal of Physical Chemistry C, 2020, 124, 27387-27395.	1.5	16
28	Nanomanufacturing of Non-Noble Amorphous Alloys for Electrocatalysis. ACS Applied Energy Materials, 2020, 3, 12099-12107.	2.5	14
29	Hydrogen oxidation reaction response of noble-metal based bulk metallic glasses. Electrochimica Acta, 2020, 353, 136616.	2.6	9
30	Functionally Graded Gecko Setae and the Biomimics with Robust Adhesion and Durability. ACS Applied Polymer Materials, 2020, 2, 2658-2666.	2.0	18
31	Energy density-enhancement mechanism and design principles for heteroatom-doped carbon supercapacitors. Nano Energy, 2020, 72, 104666.	8.2	65
32	Preaddition of Cations to Electrolytes for Aqueous 2.2 V High Voltage Hybrid Supercapacitor with Superlong Cycling Life and Its Energy Storage Mechanism. ACS Applied Materials & Interfaces, 2020, 12, 17659-17668.	4.0	27
33	Highâ€Performance, Longâ€Life, Rechargeable Li–CO <sub>2</sub> Batteries based on a 3D Holey Graphene Cathode Implanted with Single Iron Atoms. Advanced Materials, 2020, 32, e1907436.	11.1	133
34	Controllable growth of two-dimensional iron carbide in steels under accumulation deformation. Micron, 2020, 132, 102794.	1,1	1
35	Origins of Boosted Charge Storage on Heteroatomâ€Doped Carbons. Angewandte Chemie - International Edition, 2020, 59, 7928-7933.	7.2	102
36	Harnessing the interplay of Fe–Ni atom pairs embedded in nitrogen-doped carbon for bifunctional oxygen electrocatalysis. Nano Energy, 2020, 71, 104597.	8.2	231

#	Article	IF	CITATIONS
37	Editorial: Catalysts for Clean Energy Conversion and Storage. Frontiers in Materials, 2020, 7, .	1.2	2
38	Design principles of pseudocapacitive carbon anode materials for ultrafast sodium and potassium-ion batteries. Journal of Materials Chemistry A, 2020, 8, 7756-7764.	5.2	16
39	Self-Assembly of Metallo-Supramolecules under Kinetic or Thermodynamic Control: Characterization of Positional Isomers Using Scanning Tunneling Spectroscopy. Journal of the American Chemical Society, 2020, 142, 9809-9817.	6.6	14
40	Catalytic Mechanisms and Design Principles for Singleâ€Atom Catalysts in Highly Efficient CO <sub>2</sub> Conversion. Advanced Energy Materials, 2019, 9, 1902625.	10.2	167
41	Metal Coordinationâ€Mediated Functional Grading and Selfâ€Healing in Mussel Byssus Cuticle. Advanced Science, 2019, 6, 1902043.	5.6	35
42	Phase stability of an high-entropy Al-Cr-Fe-Ni-V alloy with exceptional mechanical properties: First-principles and APT investigations. Computational Materials Science, 2019, 170, 109161.	1.4	15
43	Rapid Water Harvesting and Nonthermal Drying in Humid Air by N-Doped Graphene Micropads. Langmuir, 2019, 35, 12389-12399.	1.6	6
44	Rational design of efficient transition metal core–shell electrocatalysts for oxygen reduction and evolution reactions. RSC Advances, 2019, 9, 536-542.	1.7	5
45	A self-healing hydrogel with pressure sensitive photoluminescence for remote force measurement and healing assessment. Materials Horizons, 2019, 6, 703-710.	6.4	66
46	Catalytic origin and universal descriptors of heteroatom-doped photocatalysts for solar fuel production. Nano Energy, 2019, 63, 103819.	8.2	25
47	Catalytic Activity Origin and Design Principles of Graphitic Carbon Nitride Electrocatalysts for Hydrogen Evolution. Frontiers in Materials, 2019, 6, .	1.2	50
48	Graphene-covered transition metal halide molecules as efficient and durable electrocatalysts for oxygen reduction and evolution reactions. Physical Chemistry Chemical Physics, 2019, 21, 23094-23101.	1.3	8
49	Detrimental Effects and Prevention of Acidic Electrolytes on Oxygen Reduction Reaction Catalytic Performance of Heteroatom-Doped Graphene Catalysts. Frontiers in Materials, 2019, 6, .	1.2	6
50	Controlled Surface Elemental Distribution Enhances Catalytic Activity and Stability. Matter, 2019, 1, 1447-1449.	5.0	7
51	Mussel Byssus Cuticle: Metal Coordinationâ€Mediated Functional Grading and Selfâ€Healing in Mussel Byssus Cuticle (Adv. Sci. 23/2019). Advanced Science, 2019, 6, 1970138.	5.6	1
52	Highly Switchable Adhesion of N-Doped Graphene Interfaces for Robust Micromanipulation. ACS Applied Materials & Interfaces, 2019, 11, 5544-5553.	4.0	7
53	Coordination-Dependent Catalytic Activity and Design Principles of Metal–Organic Frameworks as Efficient Electrocatalysts for Clean Energy Conversion. Journal of Physical Chemistry C, 2019, 123, 214-221.	1.5	10
54	Guiding Principles for Designing Highly Efficient Metalâ€Free Carbon Catalysts. Advanced Materials, 2019, 31, e1805252.	11.1	110

#	Article	IF	CITATIONS
55	Capacitive Enhancement Mechanisms and Design Principles of Highâ€Performance Graphene Oxideâ€Based Allâ€&olidâ€&tate Supercapacitors. Advanced Functional Materials, 2018, 28, 1706721.	7.8	27
56	Catalytic mechanism and design principles for heteroatom-doped graphene catalysts in dye-sensitized solar cells. Nano Energy, 2018, 49, 193-199.	8.2	38
57	Metal Charge Transfer Doped Carbon Dots with Reversibly Switchable, Ultra-High Quantum Yield Photoluminescence. ACS Applied Nano Materials, 2018, 1, 1886-1893.	2.4	64
58	Effect of various Ca content on microstructure and fracture toughness of extruded Mg-2Zn alloys. Journal of Alloys and Compounds, 2018, 742, 1019-1030.	2.8	35
59	Self-Cleaning and Controlled Adhesion of Gecko Feet and Their Bioinspired Micromanipulators. MRS Advances, 2018, 3, 1641-1646.	0.5	5
60	Covalent Organic Framework Electrocatalysts for Clean Energy Conversion. Advanced Materials, 2018, 30, 1703646.	11.1	309
61	Temperature-induced tunable adhesion of gecko setae/spatulae and their biomimics. Materials Today: Proceedings, 2018, 5, 25879-25893.	0.9	8
62	New Theoretical Strategy for the Correlation of Oxygen Evolution Performance and Metal Catalysts Adsorption at BiVO <sub>4</sub> Surfaces. Journal of Physical Chemistry C, 2018, 122, 25195-25203.	1.5	10
63	Electrochemical Oxygen Reduction Reaction in Alkaline Solution at a Low Overpotential on (220)-Textured Ag Surface. ACS Applied Energy Materials, 2018, 1, 4385-4394.	2.5	16
64	A Pyrolysisâ€Free Covalent Organic Polymer for Oxygen Reduction. Angewandte Chemie, 2018, 130, 12747-12752.	1.6	26
65	A Pyrolysisâ€Free Covalent Organic Polymer for Oxygen Reduction. Angewandte Chemie - International Edition, 2018, 57, 12567-12572.	7.2	120
66	Tough Reversible Adhesion Properties of a Dry Self-Cleaning Biomimetic Surface. ACS Applied Materials & Interfaces, 2018, 10, 26787-26794.	4.0	21
67	First-principles screening visible-light active delafossite ABO2 structures for photocatalytic application. International Journal of Hydrogen Energy, 2018, 43, 17271-17282.	3.8	11
68	Role of interfaces in mechanical properties of ceramic matrix composites. , 2018, , 355-374.		3
69	Design Principles for Covalent Organic Frameworks as Efficient Electrocatalysts in Clean Energy Conversion and Green Oxidizer Production. Advanced Materials, 2017, 29, 1606635.	11.1	167
70	Atomic simulations of twist grain boundary structures and deformation behaviors in aluminum. AIP Advances, 2017, 7, .	0.6	20
71	In Situ Exfoliated, Edgeâ€Rich, Oxygenâ€Functionalized Graphene from Carbon Fibers for Oxygen Electrocatalysis. Advanced Materials, 2017, 29, 1606207.	11.1	532
72	The activity origin of core–shell and alloy AgCu bimetallic nanoparticles for the oxygen reduction reaction. Journal of Materials Chemistry A, 2017, 5, 7043-7054.	5.2	60

Zhenhai Xia

#	Article	IF	CITATIONS
73	Creating coordinatively unsaturated metal sites in metal-organic-frameworks as efficient electrocatalysts for the oxygen evolution reaction: Insights into the active centers. Nano Energy, 2017, 41, 417-425.	8.2	386
74	Ag, Co/graphene interactions and its effect on electrocatalytic oxygen reduction in alkaline media. Journal of Power Sources, 2017, 370, 1-13.	4.0	19
75	Molecular dynamic simulation of nanocrystal formation and tensile deformation of TiAl alloy. RSC Advances, 2017, 7, 48315-48323.	1.7	21
76	Interactions between Dopants in Dual-Doped Graphene Nanoribbons as Metal-Free Bifunctional Catalysts for Fuel Cell and Metal-Air Batteries. MRS Advances, 2016, 1, 421-425.	0.5	2
77	Charge transfer induced activity of graphene for oxygen reduction. Nanotechnology, 2016, 27, 185402.	1.3	19
78	Biomimetic self-cleaning surfaces: synthesis, mechanism and applications. Journal of the Royal Society Interface, 2016, 13, 20160300.	1.5	86
79	Synthesis, properties and applications of 3D carbon nanotube–graphene junctions. Journal Physics D: Applied Physics, 2016, 49, 443001.	1.3	18
80	Hydrogen evolution: Guiding principles. Nature Energy, 2016, 1, .	19.8	56
81	Template-directed growth and mechanical properties of carbon nanotube–graphene junctions with nano-fillets: molecular dynamic simulation. RSC Advances, 2016, 6, 56077-56082.	1.7	2
82	Two-Dimensional Layered Oxide Structures Tailored by Self-Assembled Layer Stacking via Interfacial Strain. ACS Applied Materials & Interfaces, 2016, 8, 16845-16851.	4.0	26
83	Fabrication of TiO <sub>2</sub> –graphene composite for the enhanced performance of lithium batteries. RSC Advances, 2016, 6, 66971-66977.	1.7	9
84	Singleâ^'sided fluorine–functionalized graphene: A metal–free electrocatalyst with high efficiency for oxygen reduction reaction. Carbon, 2016, 104, 56-63.	5.4	51
85	Design Principles for Dual-Element-Doped Carbon Nanomaterials as Efficient Bifunctional Catalysts for Oxygen Reduction and Evolution Reactions. ACS Catalysis, 2016, 6, 1553-1558.	5.5	179
86	Novel insights into l-cysteine adsorption on transition metal doped graphene: influences of the dopant and the vacancy. RSC Advances, 2016, 6, 29830-29839.	1.7	7
87	Electron Transfer and Catalytic Mechanism of Organic Molecule-Adsorbed Graphene Nanoribbons as Efficient Catalysts for Oxygen Reduction and Evolution Reactions. Journal of Physical Chemistry C, 2016, 120, 2166-2175.	1.5	42
88	Hyperelastic Multi-Scale Modeling of a Thermoplastic Polyurethane Elastomer Using Molecular Mechanics. , 2015, , .		5
89	Design Principles for Heteroatomâ€Đoped Carbon Nanomaterials as Highly Efficient Catalysts for Fuel Cells and Metal–Air Batteries. Advanced Materials, 2015, 27, 6834-6840.	11.1	490
90	Role of lattice defects in catalytic activities of graphene clusters for fuel cells. Physical Chemistry Chemical Physics, 2015, 17, 16733-16743.	1.3	181

Zhenhai Xia

#	Article	IF	CITATIONS
91	A metal-free bifunctional electrocatalyst for oxygen reduction and oxygen evolution reactions. Nature Nanotechnology, 2015, 10, 444-452.	15.6	2,782
92	Rationally designed graphene-nanotube 3D architectures with a seamless nodal junction for efficient energy conversion and storage. Science Advances, 2015, 1, e1400198.	4.7	176
93	Carbon-based electrocatalysts for advanced energy conversion and storage. Science Advances, 2015, 1, e1500564.	4.7	567
94	Synthesis, mechanistic investigation, and application of photoluminescent sulfur and nitrogen co-doped carbon dots. Journal of Materials Chemistry C, 2015, 3, 9885-9893.	2.7	154
95	Robust self-cleaning and micromanipulation capabilities of gecko spatulae and their bio-mimics. Nature Communications, 2015, 6, 8949.	5.8	124
96	Correlating Electrical Resistance Change with Mechanical Damage in Woven <scp><scp>SiC</scp></scp> / <scp><scp>SiC</scp> Composites: Experiment and Modeling. Journal of the American Ceramic Society, 2014, 97, 2936-2942.</scp>	1.9	20
97	Growth of junctions in 3D carbon nanotube-graphene nanostructures: A quantum mechanical molecular dynamic study. Carbon, 2014, 67, 627-634.	5.4	46
98	N-doped graphene as catalysts for oxygen reduction and oxygen evolution reactions: Theoretical considerations. Journal of Catalysis, 2014, 314, 66-72.	3.1	537
99	Growth mechanisms and mechanical properties of 3D carbon nanotube–graphene junctions: molecular dynamic simulations. RSC Advances, 2014, 4, 33848-33854.	1.7	15
100	Strain and structure heterogeneity in MoS2 atomic layers grown by chemical vapour deposition. Nature Communications, 2014, 5, 5246.	5.8	453
101	Dynamic Adhesion Forces between Microparticles and Substrates in Water. Langmuir, 2014, 30, 11103-11109.	1.6	31
102	Fracture and toughening mechanisms in SiC nanofiber reinforced SiC matrix nanocomposites with amorphous carbon coatings. Computational Materials Science, 2014, 83, 255-260.	1.4	6
103	Catalytic Mechanisms of Sulfur-Doped Graphene as Efficient Oxygen Reduction Reaction Catalysts for Fuel Cells. Journal of Physical Chemistry C, 2014, 118, 3545-3553.	1.5	373
104	Anomalous Capacitive Behaviors of Graphene Oxide Based Solid-State Supercapacitors. Nano Letters, 2014, 14, 1938-1943.	4.5	78
105	Edge‣electively Sulfurized Graphene Nanoplatelets as Efficient Metalâ€Free Electrocatalysts for Oxygen Reduction Reaction: The Electron Spin Effect. Advanced Materials, 2013, 25, 6138-6145.	11.1	537
106	Development of CVD Ti-containing films. Progress in Materials Science, 2013, 58, 1490-1533.	16.0	38
107	Dynamic Enhancement in Adhesion Forces of Microparticles on Substrates. Langmuir, 2013, 29, 13743-13749.	1.6	28
108	Wettability of nanotextured metallic glass surfaces. Scripta Materialia, 2013, 69, 732-735.	2.6	31

#	Article	IF	CITATIONS
109	Advanced gecko-foot-mimetic dry adhesives based on carbon nanotubes. Nanoscale, 2013, 5, 475-486.	2.8	54
110	Facile, scalable synthesis of edge-halogenated graphene nanoplatelets as efficient metal-free eletrocatalysts for oxygen reduction reaction. Scientific Reports, 2013, 3, 1810.	1.6	300
111	<i>In vitro</i> and <i>in vivo</i> mechanical properties of human ulnar and median nerves. Journal of Biomedical Materials Research - Part A, 2013, 101A, 2718-2725.	2.1	52
112	Dynamic self-cleaning in gecko setae via digital hyperextension. Journal of the Royal Society Interface, 2012, 9, 2781-2790.	1.5	78
113	Molecular Dynamics Simulation of Nanoimprinting Under a High-Frequency Vibration Perturbation. Journal of Computational and Theoretical Nanoscience, 2012, 9, 35-40.	0.4	9
114	Modeling of electromechanical behavior of woven SiC/SiC composites. Composites Part A: Applied Science and Manufacturing, 2012, 43, 1730-1737.	3.8	9
115	Effect of Microstructure of Nitrogen-Doped Graphene on Oxygen Reduction Activity in Fuel Cells. Langmuir, 2012, 28, 7542-7550.	1.6	279
116	Strong Adhesion and Friction Coupling in Hierarchical Carbon Nanotube Arrays for Dry Adhesive Applications. ACS Applied Materials & Interfaces, 2012, 4, 1972-1980.	4.0	32
117	Rational Design and Nanofabrication of Geckoâ€Inspired Fibrillar Adhesives. Small, 2012, 8, 2464-2468.	5.2	44
118	BCN Graphene as Efficient Metalâ€Free Electrocatalyst for the Oxygen Reduction Reaction. Angewandte Chemie - International Edition, 2012, 51, 4209-4212.	7.2	1,119
119	Enhanced fracture toughness in carbon-nanotube-reinforced amorphous silicon nitride nanocomposite coatings. Acta Materialia, 2012, 60, 3333-3339.	3.8	29
120	Coupled thermal–mechanical modeling of carbon fibers reinforced polymer composites for damage detection. Composites Part B: Engineering, 2012, 43, 1631-1636.	5.9	8
121	Measurement of Interfacial Energy and Friction Between Carbon Nanotubes and Polymer Matrix by a Micro-Pullout Test. Science of Advanced Materials, 2012, 4, 888-892.	0.1	9
122	Membranes of Vertically Aligned Superlong Carbon Nanotubes. Langmuir, 2011, 27, 8437-8443.	1.6	119
123	Electrical Resistance as a Nondestructive Evaluation Technique for SiC/SiC Ceramic Matrix Composites Under Creepâ€Rupture Loading. International Journal of Applied Ceramic Technology, 2011, 8, 298-307.	1.1	41
124	Mechanisms of Oxygen Reduction Reaction on Nitrogen-Doped Graphene for Fuel Cells. Journal of Physical Chemistry C, 2011, 115, 11170-11176.	1.5	1,235
125	Damage detection of carbon fiber reinforced polymer composites via electrical resistance measurement. Composites Part B: Engineering, 2011, 42, 77-86.	5.9	199
126	Plasma Treated Multi-Walled Carbon Nanotubes (MWCNTs) for Epoxy Nanocomposites. Polymers, 2011, 3, 2142-2155.	2.0	24

#	Article	IF	CITATIONS
127	Fabrication of Y-junction metal nanowires by AAO template-assisted AC electrodeposition. Nano-Micro Letters, 2011, 2, 290.	14.4	1
128	Voltage-controlled flow regulating in nanofluidic channels with charged polymer brushes. Microfluidics and Nanofluidics, 2010, 9, 915-922.	1.0	40
129	Synthetic hierarchical nanostructures: growth of carbon nanofibers on microfibers by chemical vapor deposition. Materials Science and Engineering B: Solid-State Materials for Advanced Technology, 2010, 166, 190-195.	1.7	14
130	Optimizing load transfer in multiwall nanotubes through interwall coupling: Theory and simulation. Acta Materialia, 2010, 58, 6324-6333.	3.8	24
131	Fabrication of Y-junction Metal Nanowires by AAO Template-assisted AC Electrodeposition. Nano-Micro Letters, 2010, 2, 290-295.	14.4	5
132	Friction and Adhesion of Hierarchical Carbon Nanotube Structures for Biomimetic Dry Adhesives: Multiscale Modeling. ACS Applied Materials & Interfaces, 2010, 2, 2570-2578.	4.0	37
133	Mechanical behavior of anodic alumina coatings reinforced with carbon nanofibers. Journal of Materials Science, 2009, 44, 6020-6027.	1.7	9
134	Molecular Dynamics Simulations of Interfacial Sliding in Carbonâ€Nanotube/Diamond Nanocomposites. Journal of the American Ceramic Society, 2009, 92, 2331-2336.	1.9	31
135	Multiscale modeling of ductile-fiber-reinforced composites. Composites Science and Technology, 2009, 69, 1887-1895.	3.8	16
136	Nitrogen-Doped Carbon Nanotube Arrays with High Electrocatalytic Activity for Oxygen Reduction. Science, 2009, 323, 760-764.	6.0	6,535
137	Static and dynamic responses of polyelectrolyte brushes under external electric field. Nanotechnology, 2009, 20, 195703.	1.3	43
138	Damage detection via electrical resistance in CFRP composites under cyclic loading. Composites Science and Technology, 2008, 68, 2526-2534.	3.8	33
139	Multiscale Modeling of Tensile Failure in Fiber-Reinforced Composites. , 2008, , 37-82.		1
140	Carbon Nanotube Arrays with Strong Shear Binding-On and Easy Normal Lifting-Off. Science, 2008, 322, 238-242.	6.0	674
141	Modeling of Nanoimprinting of Metals by Nanotube Arrays. Materials Research Society Symposia Proceedings, 2008, 1137, 101301.	0.1	0
142	Enhancing Mechanical Properties of Multiwall Carbon Nanotubes viasp3Interwall Bridging. Physical Review Letters, 2007, 98, 245501.	2.9	108
143	Synthesis and Properties of Cobalt Nanowires. , 2007, , .		0
144	Modeling of mechanical damage detection in CFRPs via electrical resistance. Composites Science and Technology, 2007, 67, 1518-1529.	3.8	52

#	Article	IF	CITATIONS
145	Shell Buckling of Imperfect Multiwalled Carbon Nanotubes—Experiments and Analysis. Experimental Mechanics, 2007, 47, 153-161.	1.1	15
146	Mechanism of Horizontally Aligned Growth of Single-Wall Carbon Nanotubes on R-Plane Sapphire. Journal of Physical Chemistry B, 2006, 110, 22676-22680.	1.2	58
147	Multiscale Modeling of Frictional Behavior of Highly-Ordered Carbon Nanotube/Ceramic Nanocomposites. Materials Research Society Symposia Proceedings, 2006, 978, .	0.1	0
148	Multiscale Modeling of Carbon Nanotube Adhesion for Dry Adhesives. Materials Research Society Symposia Proceedings, 2006, 975, 1.	0.1	2
149	Fracture Toughness of Highly Ordered Carbon Nanotube/Alumina Nanocomposites. Journal of Engineering Materials and Technology, Transactions of the ASME, 2004, 126, 238-244.	0.8	52
150	Direct observation of toughening mechanisms in carbon nanotube ceramic matrix composites. Acta Materialia, 2004, 52, 931-944.	3.8	430
151	A new method to evaluate the fracture toughness of thin films. Acta Materialia, 2004, 52, 3507-3517.	3.8	88
152	Quantitative damage detection in CFRP composites. Composites Science and Technology, 2003, 63, 1411-1422.	3.8	71
153	Shear-lag versus finite element models for stress transfer in fiber-reinforced composites. Composites Science and Technology, 2002, 62, 1141-1149.	3.8	78
154	Green's function vs. shear-lag models of damage and failure in fiber composites. Composites Science and Technology, 2002, 62, 1279-1288.	3.8	54
155	Multiscale modeling of damage and failure in aluminum-matrix composites. Composites Science and Technology, 2001, 61, 2247-2257.	3.8	39
156	Multiscale modeling of failure in metal matrix composites. Acta Materialia, 2001, 49, 273-287.	3.8	92
157	Life prediction of titanium MMCs under low-cycle fatigue. Acta Materialia, 2001, 49, 1633-1646.	3.8	14
158	Tough-to-brittle transitions in ceramic-matrix composites with increasing interfacial shear stress. Acta Materialia, 2000, 48, 4879-4892.	3.8	71
159	Finite element modelling of fatigue crack initiation in SiC-fibre reinforced titanium alloys. Composites Part A: Applied Science and Manufacturing, 2000, 31, 1031-1037.	3.8	16
160	Fabrication of laminated metal–intermetallic composites by interlayer in-situ reaction. Journal of Materials Science, 1999, 34, 3731-3735.	1.7	19
161	Fabrication of fiber-reinforced metal-matrix composites by variable pressure infiltration. Metallurgical and Materials Transactions B: Process Metallurgy and Materials Processing Science, 1992, 23, 295-302.	1.0	16
162	Design of FiberCoating Systems for High Strength in Ceramic Matrix Composites. , 0, , 371-378.		4

Design of FiberCoating Systems for High Strength in Ceramic Matrix Composites. , 0, , 371-378. 162

#	Article	IF	CITATIONS
163	Core Effect of Local Atomic Configuration and Design Principles of Al <sub>x</sub> CoCrFeNi High-Entropy Alloys. SSRN Electronic Journal, 0, , .	0.4	Ο